

# Optimal amplification of the dynamical Casimir effect in a parametrically driven system

Fabian Hoeb,<sup>1</sup> Fabrizio Angaroni,<sup>2,3</sup> Jonathan Zoller,<sup>1</sup> Tommaso Calarco,<sup>1</sup>  
Giuliano Strini,<sup>4</sup> Simone Montangero,<sup>5,1</sup> and Giuliano Benenti<sup>2,3,6</sup>

<sup>1</sup>*Institute for Complex Quantum Systems & Center for Integrated Quantum Science and Technology (IQST),  
Ulm University, Albert-Einstein-Allee 11, D-89069 Ulm, Germany*

<sup>2</sup>*Center for Nonlinear and Complex Systems, Dipartimento di Scienza e Alta Tecnologia,  
Università degli Studi dell'Insubria, via Valleggio 11, 22100 Como, Italy*

<sup>3</sup>*Istituto Nazionale di Fisica Nucleare, Sezione di Milano, via Celoria 16, 20133 Milano, Italy*

<sup>4</sup>*Department of Physics, University of Milan, via Celoria 16, 20133 Milano, Italy*

<sup>5</sup>*Theoretische Physik, Universität des Saarlandes, D-66123 Saarbrücken, Germany*

<sup>6</sup>*NEST, Istituto Nanoscienze-CNR, 56126 Pisa, Italy*

We introduce different strategies to enhance photon generation in a cavity within the Rabi model in the ultrastrong coupling regime. We show that a bang-bang strategy allows to enhance the effect of up to one order of magnitude with respect to simply driving the system in resonance for a fixed time. Moreover, up to about another order of magnitude can be gained exploiting quantum optimal control strategies. Finally, we show that such optimized protocols are robust with respect to systematic errors and noise, paving the way to future experimental implementations of such strategies.

PACS numbers: 42.50.Lc, 42.50.Dv, 03.67.-a

## I. INTRODUCTION

High-speed manipulation of quantum systems is key in quantum information processing: Quantum gates should operate on a time scale much smaller than the decoherence time, to allow efficient error correction and fault-tolerant architectures [1–3]. Similarly, the transmission rate is a fundamental characteristic to assess the efficiency and the feasibility of real-world application of quantum cryptography [4–6]. Circuit quantum electrodynamics [7, 8] might play a prominent role to speed up quantum protocols, since it allows to address the ultrastrong coupling regime [9–13] of light-matter interaction, where the coupling strength  $\lambda$  becomes comparable to, or even exceeds the resonator frequency  $\omega$ . This regime has also interesting properties on its own, such as the emergence of a strongly correlated light-matter ground state [12, 13].

A related problem is the detection of the dynamical Casimir effect (DCE), namely the generation of photons from the vacuum due to time-dependent boundary conditions or, more generally, as a consequence of the nonadiabatic change of some parameters of a system [14–17]. Indeed, a rapid variation of the matter-field coupling is needed to implement ultrafast quantum gates, and therefore the DCE appears as a fundamental limit to the implementation of high-speed quantum gates [18] and more generally to the development of ultrafast quantum technologies. First experimental demonstrations of the DCE have been reported in superconducting circuit quantum electrodynamics [19, 20]. However, it is of great interest to have the ability to either enhance or counteract [18] this effect: On the one hand, it improves our capability of investigating fundamental effects in nature, and, on the other hand, it enables us to push the limits of quantum

information processing.

Here, we present three different strategies to amplify and thus improve the visibility of the DCE in a parametrically driven system via precisely tailored timing of the matter-field interaction. In detail, we consider on-off resonance sweeping of a parametrically driven qubit coupled to a single mode of the electromagnetic field. We model the qubit-field interaction by the Rabi Hamiltonian [21], with a time-dependent modulation of the qubit frequency. We use and compare two strategies to optimize the visibility of the DCE: a multi step heuristic method employing bang-bang switches of the qubit frequency from the off-resonance regime to the resonance regime and back out of resonance, and optimal control theory which has been proven to be able to successfully control circuit quantum electrodynamics processes [2, 22–28]. In particular, we employ the dressed chopped random basis algorithm (dCRAB) which has been already applied successfully to various theoretical and experimental atomic and condensed matter control problems to meet various control goals, including state-transfer, gate synthesis, observable control, and fast quantum phase transition crossing [29–35]. For the problem studied here, the control function is the time-dependent modulation of the qubit frequency and the figure of merit is the expectation value of the number of photons that are generated in the cavity by parametric amplification of the DCE: This amounts to finding an optimal setup for the detection of the DCE. The results obtained from the dCRAB algorithm are compared to the bang-bang strategy and it is shown that dCRAB could identify pulses yielding up to about one order of magnitude more photons than the bang-bang strategy and up to two orders of magnitude more photons than an unoptimized protocol, which is a single sweep of the qubit to resonance.

The manuscript is organized as follows: First, we introduce the dynamical system model in Sec. II. In Sec. III we describe the three control strategies employed to enhance the DCE, discuss the results and give an outlook towards their experimental implementation also investigating their robustness against some possible experimental imperfections. We conclude our work in Sec. IV.

## II. THE MODEL

Hereafter, we describe the interaction between a single qubit and a single mode of the quantized field by means of the Rabi Hamiltonian [21], with a time-dependent modulation:

$$H(t) = H_0(t) + H_I,$$

$$H_0(t) = -\frac{1}{2} [\omega_{q0} + \dot{\Phi}(t)] \sigma_z + \omega \left( a^\dagger a + \frac{1}{2} \right), \quad (1)$$

$$H_I = \lambda \sigma_+ (a^\dagger + a) + \lambda^* \sigma_- (a^\dagger + a),$$

where the reduced Planck's constant is set to  $\hbar = 1$ ,  $\omega_{q0}$  being the reference frequency for the qubit,  $\sigma_i$  ( $i = x, y, z$ ) are the Pauli matrices, written in the  $\{|g\rangle, |e\rangle\}$  basis;  $\sigma_\pm = \frac{1}{2} (\sigma_x \mp i\sigma_y)$  are the raising and lowering operators for the qubit (so that  $\sigma_+ = |e\rangle\langle g|$  and  $\sigma_- = |g\rangle\langle e|$ ):  $\sigma_+|g\rangle = |e\rangle$ ,  $\sigma_+|e\rangle = 0$ ,  $\sigma_-|g\rangle = 0$ ,  $\sigma_-|e\rangle = |g\rangle$ . The operators  $a^\dagger$  and  $a$  for the field create and annihilate a photon:  $a^\dagger|n\rangle = \sqrt{n+1}|n+1\rangle$ ,  $a|n\rangle = \sqrt{n}|n-1\rangle$ ,  $|n\rangle$  being the Fock state with  $n$  photons. For the sake of simplicity, we consider a real coupling strength,  $\lambda \in \mathbb{R}$ . The real function  $\dot{\Phi}(t)$  is the control field which allows to manipulate the system: the qubit frequency is modulated via  $\omega_q(t) = \omega_{q0} + \dot{\Phi}(t)$ . Notice that we used the notation with the first derivative because, as it will become apparent in the next paragraph, the relevant quantity is the accumulated phase, i.e.  $\Phi(t)$ .

The Rotating Wave Approximation (RWA) (valid for  $\lambda \rightarrow 0$ ) is obtained neglecting the term  $\sigma_+ a^\dagger$ , which simultaneously excites the qubit and creates a photon, and  $\sigma_- a$ , which de-excites the qubit and annihilates a photon. In this limit, the Hamiltonian (1) reduces to the Jaynes-Cummings Hamiltonian [21] with a time-dependent modulation. In the RWA the swapping time needed to transfer an excitation from the qubit to the field or vice versa ( $|e\rangle|0\rangle \leftrightarrow |g\rangle|1\rangle$ ) is  $\tau_s = \pi/2\lambda$ , and no DCE is possible since the total number of excitations in the system is conserved.

In the interaction picture, we first consider the unitary operator

$$U(t) = \mathcal{T} \exp \left[ -i \int_0^t d\tau H_0(\tau) \right] \\ = \mathcal{T} \exp \left\{ \frac{i}{2} [\omega_{q0} t + \Phi(t)] \sigma_z - i\omega t \left( a^\dagger a + \frac{1}{2} \right) \right\}, \quad (2)$$

where  $\mathcal{T}$  is the time-ordering operator and  $\Phi(t) = \int_0^t d\tau \dot{\Phi}(\tau)$  the accumulated phase. The time-dependent

Hamiltonian in the interaction picture then reads

$$\tilde{H}_I(t) = U^\dagger(t) H_I U(t) \\ = \lambda (a\sigma_- \exp\{-i[(2\omega - \Delta_0)t + \Phi(t)]\} \\ + a\sigma_+ \exp\{i[-\Delta_0 t + \Phi(t)]\} \\ + a^\dagger \sigma_- \exp\{-i[-\Delta_0 t + \Phi(t)]\} \\ + a^\dagger \sigma_+ \exp\{i[(2\omega - \Delta_0)t + \Phi(t)]\}), \quad (3)$$

where we have defined the reference detuning  $\Delta_0 = \omega - \omega_{q0}$ . The standard Rabi model is recovered for the time-independent Hamiltonian,  $\Phi(t) = 0$ , and the Jaynes-Cummings model if we further neglect the counter-rotating terms at frequency  $2\omega$ . From now on we will omit tildes and always refer to the interaction picture.

If we expand, in the interaction picture, the qubit-field state at time  $t$  as  $|\Psi(t)\rangle = \sum_{l=g,e} \sum_{n=0}^{\infty} C_{l,n}(t) |l, n\rangle$ , we obtain the equations that govern the evolution of the coefficients  $C_{l,n}(t)$ :

$$\begin{cases} i\dot{C}_{g,n}(t) = \Omega_n e^{-i[-\Delta_0 t + \Phi(t)]} C_{e,n-1}(t) \\ \quad + \Omega_{n+1} e^{-i[(2\omega - \Delta_0)t + \Phi(t)]} C_{e,n+1}(t), \\ i\dot{C}_{e,n}(t) = \Omega_{n+1} e^{i[-\Delta_0 t + \Phi(t)]} C_{g,n+1}(t) \\ \quad + \Omega_n e^{i[(2\omega - \Delta_0)t + \Phi(t)]} C_{g,n-1}(t). \end{cases} \quad (4)$$

Here  $\Omega_n = \lambda\sqrt{n}$  are the Rabi frequencies, with  $n = 0, 1, 2, \dots$  (the terms  $C_{l,m}$  and  $\dot{C}_{l,m}$  must be set to zero when  $m < 0$ ). In numerical simulations we will set the reference detuning  $\Delta_0 = 0$  to ensure that the off resonance condition  $|\omega - \omega_q| \ll \lambda$  holds in the ultrastrong coupling regime [9].

## III. RESULTS

We consider the time evolution of the qubit-oscillator system for an overall time interval  $T$ . An initial and a final time interval  $\tau$ , corresponding to off-resonance evolutions with detuning  $|\omega - \omega_q(t)| \gg \lambda$ , are excluded from manipulation to determine the figure of merit. Consequently, on-off resonance sweeps (governed by a time-dependent pulse  $\omega_q(t)$ ) are possible during the intermediate time span  $\tau_p = T - 2\tau$ . Initially both the field and the qubit are prepared in their ground state  $|\Psi(t=0)\rangle = |g, 0\rangle$ , so that within the RWA there is no generation of photons at all times ( $\langle n \rangle = 0 \forall t$ ). On the other hand, when the terms beyond the RWA are taken into account, only a very weak photon generation is possible in the off-resonance regime, while a significant photon emergence is possible if the resonance condition is approached nonadiabatically. To quantify the strength of this manifestation of the DCE effect, we consider the figure of merit

$$f = \bar{n}_f - \bar{n}_i, \quad (5)$$

where  $\bar{n}_{f/i} = \int \langle n(t) \rangle dt$  is the time-average of the mean photon number  $\langle n \rangle$  over the initial (i) and final (f) off-resonance time intervals of duration  $\tau$  each. Hereafter,

we set the off-resonance condition to  $\omega_q = 4\omega$ ; the exact numerical value has, however, a very minor influence only.

### A. On-off protocol

We begin by studying the efficiency of a straightforward protocol, namely a sudden switch to resonance  $\omega_q = \omega$  at time  $\tau$ , followed by another instantaneous quench to the off-resonance condition at time  $T - \tau$ . That is, the system is kept on resonance for a total time  $\tau_p$ .

Typical examples of time evolutions of the instantaneous average number of generated photons  $\langle n \rangle$  are shown in Fig. 1 (top), in the ultra-strong coupling regime, for  $\lambda = 0.80$  (solid line) and  $\lambda = 0.83$  (dashed line): it is clearly visible that the number of photons remains quite small in the initial off-resonance regime ( $t < \tau$ ), while  $\langle n \rangle$  grows rapidly after switching to the resonance condition (at time  $t = \tau = 4\tau_s$ ). It can be clearly seen that at resonance  $\langle n \rangle$  does not grow indefinitely, but oscillates due to coherent generation (dynamical Casimir effect) and destruction of photons (anti-dynamical Casimir effect [36]). Finally, after the switch to the off-resonance regime (at time  $t = T - \tau = 16\tau_s$ ), the average photon number keeps on oscillating around its value at  $t = T - \tau$  with smaller amplitude oscillations compared to the ones on resonance. In Fig. 1 (bottom) the results of this protocol are summarized, reporting the value of the figure of merit  $f$  given by Eq. (5) versus  $\lambda$ . Note that this protocol reveals a strong sensitivity with respect to variations of the system parameters, especially in the regime  $\lambda \gtrsim 0.6$  where a non negligible number of photons in the cavity are generated. Indeed, a slight change of the coupling strength  $\lambda$  induces a strong variation of the mean number of photons: For instance, in the cases reported in Fig. 1 (top) we obtain  $f \approx 0.37$  for  $\lambda = 0.80$  whereas  $f \approx 0.016$  for  $\lambda = 0.83$ . Such a strong sensitivity suggests that accurate control of the system parameters is needed for reliable implementation of quantum protocols in the ultrastrong coupling regime.

### B. Optimized strategies

In order to amplify and improve the visibility of the DCE, more sophisticated pulses with multiple on-off resonance sweeps are required. Hereafter we will implement and compare two methods, a bang-bang strategy [37] and optimal control using dCRAB [38, 39].

For the bang-bang strategy, the qubit is placed in-out resonance with instantaneous sweeps. The main idea of this strategy is pretty straightforward: the duration of the on-resonance intervals ( $\omega_q = \omega$ ) is determined by the time needed to reach the first maximum in the number of photons, while the detuned intervals ( $\omega_q = 4\omega$ ) last for a fixed time  $\tau_O \ll \tau_p$  since gain in  $f$  is mainly seen on resonance. This strategy already provides an

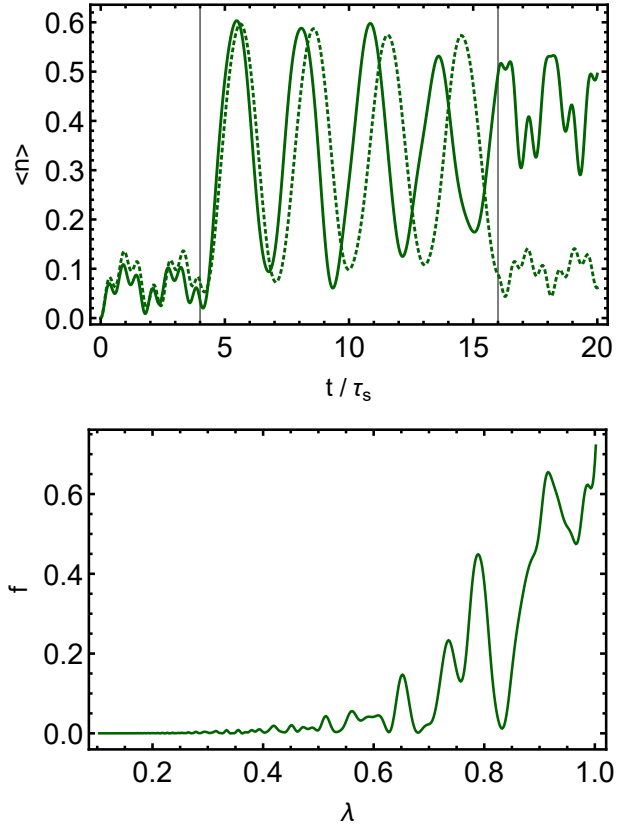


FIG. 1: Results for the on-off protocol. Top: Dynamical evolution of the mean number of photons  $\langle n \rangle$  at interaction strength  $\lambda = 0.80$  (solid green line) and  $\lambda = 0.83$  (dashed green line). Bottom: Figure of merit  $f$  as a function of the coupling strength  $\lambda$ . For both figures, the initial and final off-resonance periods, as indicated by the vertical black lines, are set to  $\tau = 4\tau_s$ .

improvement with respect to the on-off protocol (data not shown), however we are going one step further and employ a more sophisticated strategy, which makes use of multiple iterations steps, to obtain best possible on-resonance time interval lengths (for details see Appendix A).

The second approach to target the objective  $f$  is by means of the dCRAB optimal control technique [38]. The two main ingredients of dCRAB are an expansion of the control functions over a randomized truncated basis, and iterative re-initialization of local searches allowing the algorithm to escape from false traps [38, 39]: The basis functions, which define the subspace subject to search, are updated at each re-initialization step and the new emerging search directions are explored by means of gradient-free minimization algorithms.

Two representative results for coupling strengths  $\lambda = 0.17$  ( $\lambda = 0.83$ ) are presented in Fig. 2a,c (Fig. 2b,d) com-

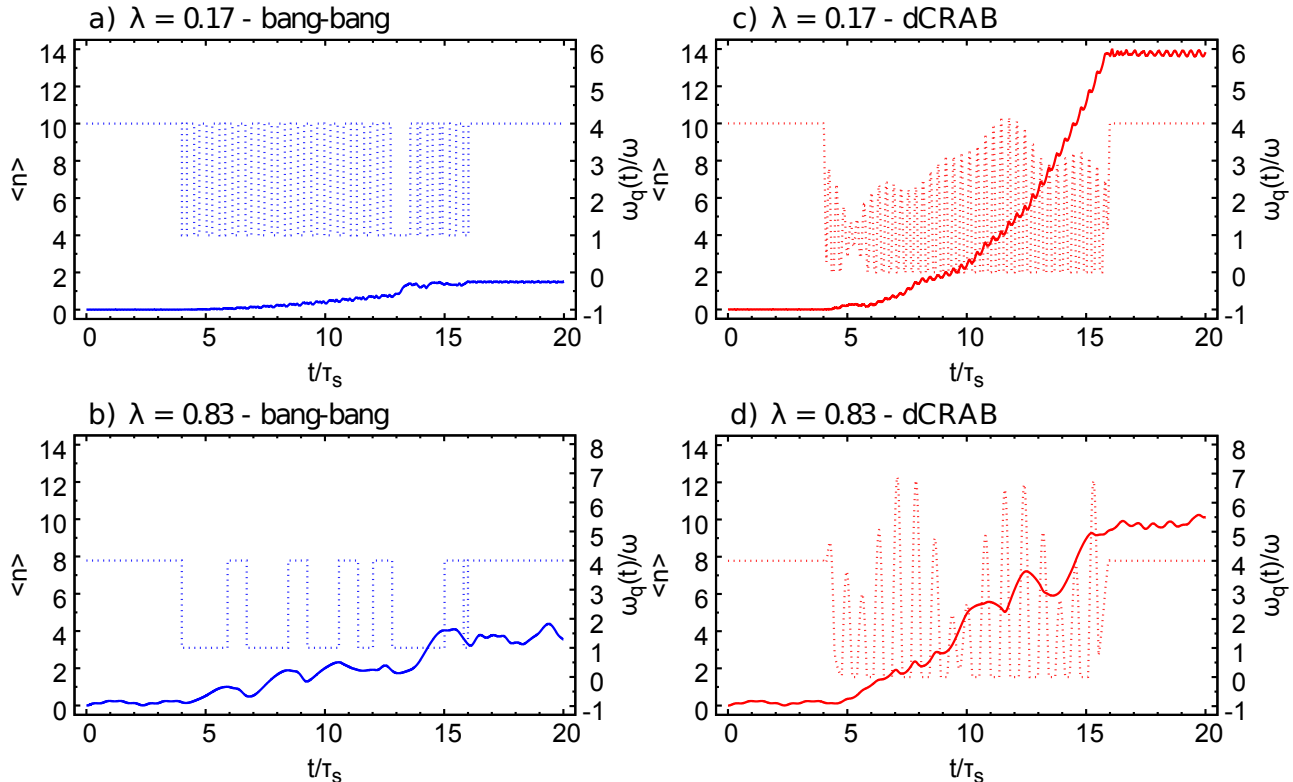


FIG. 2: Expected photon number  $\langle n \rangle$  versus time for bang-bang strategy (left, blue solid lines) and dCRAB (right, red solid lines) for coupling strengths  $\lambda = 0.17$  (a,c) and  $\lambda = 0.83$  (b,d). On the secondary y-axis, the control pulses (dashed lines, colors respectively) are displayed. Note that there is an initial and final time interval equally out of resonance for both strategies, used to compute the figure of merit  $f$  (see Eq. (5)).

paring the dCRAB solution to the outcome of the bang-bang strategy: the expectation values of the photon number are reported along with the generating control pulses  $\omega_q(t)/\omega$ . From these exemplary cases, the working principle of the bang-bang strategy is clearly revealed: Once the photon number peaks to a new maximum, the qubit frequency is driven out of resonance to let the system settle for some pre-defined time until it is switched back on resonance (see, e.g., Fig. 2b). On the contrary, for the dCRAB solution the interplay between  $\langle n \rangle$  and the control input is no longer apparent. However, it can be seen that, after some time, the number of photons generated via the dCRAB pulse always exceeds the bang-bang photons number (this is true for all cases tested). Notice that the non-negativity condition ( $\omega_q(t) \geq 0$ ) for the pulses is imposed at all times, preventing a swap in the computational basis of the qubit.

The results for different coupling strengths  $\lambda$  are summarized in Fig. 3, where the protocol's performances are clearly visible. Overall, in the ultrastrong coupling regime the improvement from the dCRAB optimizations over the bang-bang strategy is of up to one order of magnitude; compared to the unoptimized single on-off res-

onance protocol, the optimal solutions yield up to two orders of magnitudes more photons. We also tested the regime with coupling  $\lambda \ll 1$ : For  $\lambda = 0.03$ , dCRAB leads to a figure of merit  $f \approx 12$ , whereas the other two strategies perform very poorly ( $f$  well below 0.2). Quite interestingly, the dCRAB strategy shows that amplification of the DCE with a significant photon production is also possible for  $\lambda \ll 1$ , at the price of a longer duration of the protocol,  $T = 20\tau_s \propto 1/\lambda$ .

Finally, we point out that the optimal pulses identified here are expected to work equally well in a (reasonable) noisy environment, due to their intrinsic robustness against small variations, as it has been already theoretically and experimentally showed in many different scenarios [28, 40–44]. Moreover, if closed loop optimal control is employed, the optimization incorporates unknown and unpredictable drifts into the pulse design as well as makes the pulses robust against statistical disturbances (noise on the pulses and the figure of merit) [33, 41, 43]. Indeed, we could confirm the robustness of the optimal strategies by numerical simulations of the system evolution steered by the optimized dCRAB pulse (from Fig. 3d) and additionally affected by either systematic or sta-

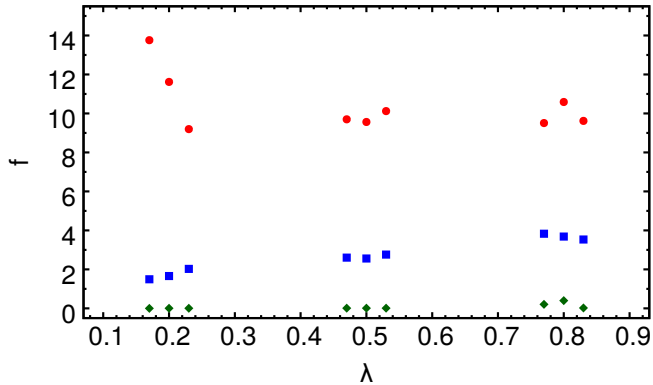


FIG. 3: Created photon number  $f$  versus coupling strength  $\lambda$  after application of three different control strategies: dCRAB optimization (red circles), bang-bang strategy (blue squares) and unoptimized on/off resonance sweeps (green diamonds). Note that the dCRAB optimized solutions improve significantly compared to the other two strategies and hence pave the way towards optimal amplification of the DCE.

tistical errors. In the former case, we assume the presence of a systematic error in the coupling strength compared to one specific coupling strength that was used in the optimization. For the analysis shown in Fig. 4 (top), we choose  $\lambda = 0.83$  as the reference strength for the optimization and show the outcome  $f$  for different values of  $\lambda \in (0.80, 0.86)$ . We can conclude that for the tested range, the figure of merit  $f$  still remains reasonably good (more than  $2/3$  of the optimized  $f$ ), and anyway much bigger than what could be obtained with the other strategies. Moreover, notice that the region of this particular coupling strength is highly sensitive in terms of photon generation as we could see for the on-off protocol in Fig. 1: For instance, going from  $\lambda = 0.80$  to  $\lambda = 0.83$ , means a drop in  $f$  by a factor of more than 20 for the unoptimized protocol.

Finally, we analyze the scenario where the optimal pulse  $\omega_q(t)$  is affected by random noise  $\xi(t)$  uniformly distributed in the interval  $[-\delta\omega, \delta\omega]$ . In Fig. 4 (bottom), we can see that the figure of merit  $f$  (averaged over 100 noise realizations) is very stable in the range  $\delta\omega/\omega = [0, 0.4]$  and was fitted to scale as  $f(\delta\omega) = (9.62 \pm 0.00494) - (0.174 \pm 0.0633) \cdot \delta\omega^2$ . The correlation time of the noise was set to be  $\tau_c = 0.03T$ , however we checked over about three orders of magnitude that it does have an almost negligible effect only (data not shown).

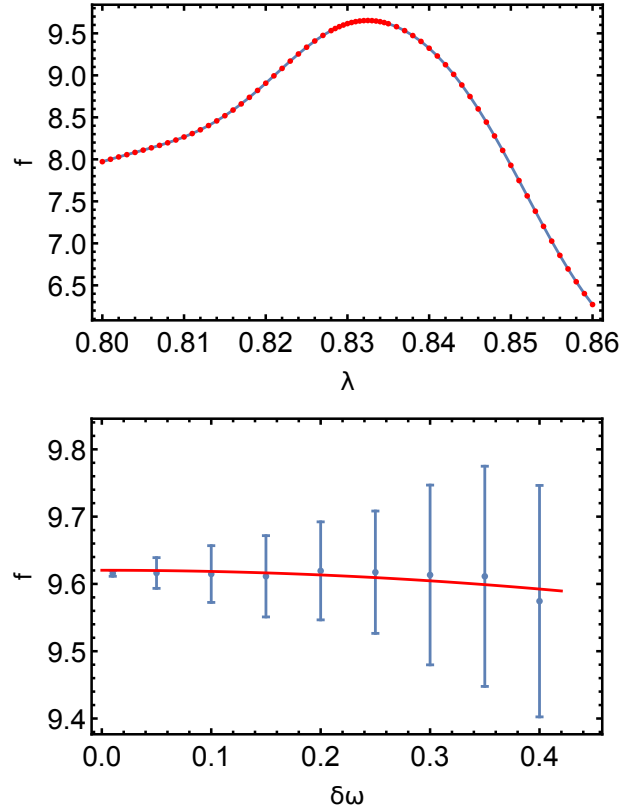


FIG. 4: Figure of merit for the dCRAB pulse computed for the unperturbed  $\lambda = 0.83$  case, when the system is exposed either to a systematic (top) or statistical (bottom) errors. In the former case, the actual value of  $\lambda$  set for the propagation ranges in  $(0.80, 0.86)$ . In the latter, the qubit frequency  $\omega_q(t)$  is affected by random noise uniformly distributed in the interval  $[-\delta\omega, \delta\omega]$ , with correlation time  $\tau_c \approx 0.03T$ . That is,  $\xi(t)$  is reset every time interval  $\tau_c$ . Error bars denote statistical errors for 100 realizations of noise per point, while the red straight line shows the outcome from a quadratic fit.

#### IV. CONCLUSIONS

We have applied different optimization strategies to a driven Rabi model Hamiltonian in the ultrastrong coupling regime. In particular, we have optimized the number of photons generated by the dynamical Casimir effect, in order to enhance its visibility in view of possible future experimental verifications. The huge amplification of the DCE given by the dCRAB optimization is quantified by an enhancement of the generated photons of up to about an order of magnitude with respect to a reference bang-bang strategy and of up to about two orders of magnitude with respect to the unoptimized on-off strategy.

The optimization performed in this paper is a valid proof of concept. Moreover, the parameters used in

our simulations are within reach for present technology, where coupling strengths even exceeding the resonator frequency have been recently reported [12, 13]. Additionally, in circuit quantum electrodynamics experiments the populations of Fock and coherent states were measured by means of the Fourier transform of the time-dependent polarization signal of a probe qubit interacting with the field [45]; extensions of this method [46] would allow not only the detection of the number of photons but also the reconstruction of the exotic field states generated by the DCE [47]. More realistic models would need a detailed treatment of decoherence sources and experimental imperfections, e.g. in driving the matter-field coupling or measuring the final state of the system. Hence, given that our results have been obtained for an idealized scenario, they are an estimate of the upper bound of the strength of the DCE in the driven Rabi model. However, as we have shown that optimal solutions are robust with respect to noise sources and systematic errors, we are optimistic about the possible experimental verification of the presented results in the future.

Finally, the same approach can be used to prepare and investigate different states and phenomena in the ultra-strong coupling regime, as for example, targeting a given Fock state of the field or generating squeezed field states.

We acknowledge support from the EU via the RYSQ project and from the DFG via the SFB/TRR21 and from BMBF via the project Q.Com. S.M. gratefully acknowledges the support of the DFG via a Heisenberg fellowship.

## Appendix A: Optimized Bang-bang strategy

We build optimized pulses employing bang-bang switches from an off resonance regime, where  $\omega_q = 4\omega$ , to the resonance regime  $\omega_q = \omega$  and back out of resonance after some fixed time  $\tau_O$ . The pulses have a total duration of  $T = 20 \cdot \tau_s$ , however we reserve an initial and final  $\tau$  where the pulse is kept constant to compute  $\bar{n}_{f/i}$  to determine the figure of merit  $f$  in Eq. (5).

To optimize the pulses the system is firstly evolved according to an initial single bang-bang pulse  $\omega_{q,ref}^{(0)}$  (dashed line in Fig. 5 a)), which is iteratively improved according to the following procedure:

- 1):** Evaluate the time evolution for the pulse  $\omega_{q,ref}^{(i)}$  and locate the first local maximum of photon number  $\langle n_M(t_M^{(i)}) \rangle$  after the last switch to resonance in the current pulse.
- 2):** Generate a new pulse  $\omega_{q,ref}^{(i+1)}$  based on  $\omega_{q,ref}^{(i)}$  by switching out of resonance at  $t_M^{(i)}$  (point in time of first occurring maximum in considered time interval). Remain out of resonance for some initially specified time  $\tau_O$ . Finally, at  $t_M^{(i)} + \tau_O$ , the pulse reverts back to resonance for the remaining  $t \in (t_M^{(i)} + \tau_O, T - \tau)$ .

**3):** At  $t = T - \tau$  switch back off-resonance to allow for the computation of the figure of merit  $f$ .

**4):** Iterate steps 1) - 3) and stop when  $t_M^{(i)} > T - \tau$ .

In Fig. 5 we show a typical result of the first iteration of this strategy: It can be clearly seen that after going on resonance the photon number rapidly increase and stabilizes to a higher value. The introduction of a non negligible off-resonance time period  $\tau_O$  leads to generally better results by letting the system equilibrate to the new conditions.

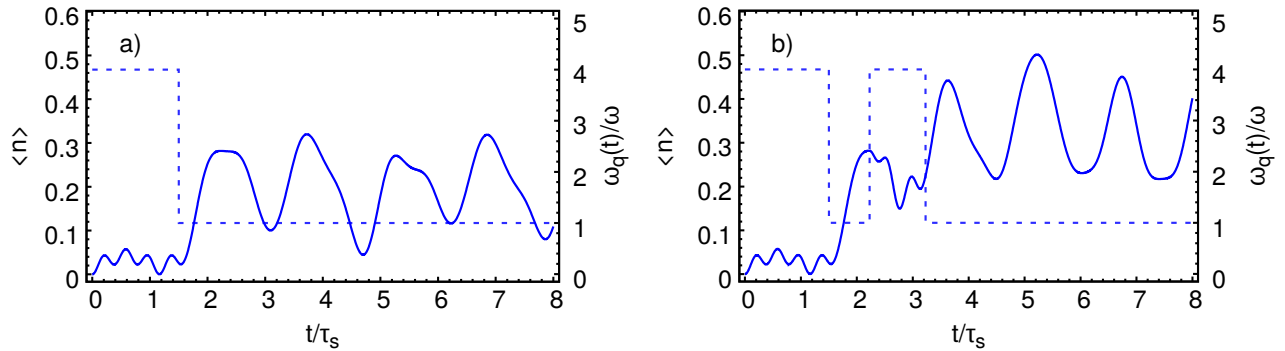


FIG. 5: Working principle of the bang-bang strategy shown for an initial pulse (a) and the first iteration of the algorithm (b), for  $\lambda = 0.5$  and  $\tau_O/\tau_s = 1.5$ . During the time on resonance of the pulse (dashed line in a))  $\langle n \rangle (t)$  oscillates around an average value (solid line in a)). Upon switching back out of resonance at the maximum of the first oscillation (the corresponding pulse is the dashed line in b)), the values of  $\langle n \rangle$  remains almost frozen around this maximum (solid line in b)). Reverting back to the resonance regime leads to the oscillatory behavior of  $\langle n \rangle$ . The initial fast increase after each switch on resonance results in the overall population increase of the cavity.

- 
- [1] T. D. Ladd, F. Jelezko, R. Laflamme, Y. Nakamura, C. Monroe, and J. O'Brien *Nature* **464**, 45 (2010).
- [2] S. J. Glaser, U. Boscain, T. Calarco, C. P. Koch, W. Köckenberger, R. Kosloff, I. Kuprov, B. Luy, S. Schirmer, T. Schulte-Herbrüggen, D. Sugny, and F. K. Wilhelm *Eur. Phys. J. D* **69**, 279 (2015).
- [3] T. Caneva, M. Murphy, T. Calarco, R. Fazio, S. Montangero, V. Giovannetti, and G. E. Santoro, *Phys. Rev. Lett.* **103**, 240501 (2009).
- [4] N. Gisin, G. Ribordy, W. Tittel, and Hugo Zbinden, *Rev. Mod. Phys.* **74**, 145 (2002).
- [5] V. Scarani, Helle Bechmann-Pasquinucci, N. J. Cerf, M. Dušek, N. Lütkenhaus, and M. Peev, *Rev. Mod. Phys.* **81**, 1301 (2009).
- [6] H.-K. Lo, M. Curty, and K. Tamaki, *Nature Photonics* **8**, 595 (2014).
- [7] A. Blais, R.-S. Huang, A. Wallraff, S. M. Girvin, and R. J. Schoelkopf, *Phys. Rev. A* **69**, 062320 (2004).
- [8] A. Wallraff, D. I. Schuster, A. Blais, L. Frunzio, R.-S. Huang, J. Majer, S. Kumar, S. M. Girvin, and R. J. Schoelkopf, *Nature* **431**, 162 (2004).
- [9] J. Bourassa, J. M. Gambetta, A. A. Abdumalikov, Jr., O. Astafiev, Y. Nakamura, and A. Blais, *Phys. Rev. A* **80**, 032109 (2009).
- [10] T. Niemczyk, F. Deppe, H. Huebl, E. Menzel, F. Hocke, M. J. Schwarz, J. J. García-Ripoll, D. Zueco, T. Hümmer, E. Solano, A. Marx, and R. Gross, *Nature Phys.* **6**, 772 (2010).
- [11] P. Forn-Díaz, J. Lisenfeld, D. Marcos, J. J. García-Ripoll, E. Solano, C. J. P. M. Harmans, and J. E. Mooij, *Phys. Rev. Lett.* **105**, 237001 (2010).
- [12] P. Forn-Díaz, J. J. García-Ripoll, B. Peropadre, J.-L. Orgiazzi, M. A. Yurtalan, R. Belyansky, C. M. Wilson, and A. Lupascu, *Nature Phys.* **13**, 39 (2017).
- [13] F. Yoshihara, T. Fuse, S. Ashhab, K. Kakuyanagi, S. Saito, and K. Semba, *Nature Phys.* **13**, 44 (2017).
- [14] G. T. Moore, *J. Math. Phys. (N.Y.)* **11**, 2679 (1970).
- [15] V. V. Dodonov, *Phys. Scripta* **82**, 038105 (2010).
- [16] P. D. Nation, J. R. Johansson, M. P. Blencowe, and F. Nori, *Rev. Mod. Phys.* **84**, 1 (2012).
- [17] The phenomena where the photons are created by parametric amplification of vacuum fluctuations without moving boundaries is referred to as parametric DCE [15]. This is the case for the driven Rabi Hamiltonian discussed in this paper.
- [18] G. Benenti, A. D'Arrigo, S. Siccardi, and G. Strini, *Phys. Rev. A* **90**, 052313 (2014).
- [19] C. M. Wilson, G. Johansson, A. Pourkabirian, M. Simoen, J. R. Johansson, T. Duty, F. Nori, and P. Delsing, *Nature (London)* **479**, 376 (2011).
- [20] P. Lähteenmäki, G. S. Paraoanu, J. Hassel, and P. J. Hakonen, *PNAS* **110**, 4234 (2013).
- [21] P. Meystre and M. Sargent III, *Elements of quantum optics* (4th Ed.) (Springer-Verlag, Berlin, 2007).
- [22] C. Brif, R. Chakrabarti, and H. Rabitz, *New J. Phys.* **12**, 75008 (2010).
- [23] M. H. Goerz, F. Motzoi, K. B. Whaley, and C. P. Koch [arXiv:1606.08825](https://arxiv.org/abs/1606.08825).
- [24] C. P. Koch, *J. Phys. Condens. Matter* **28**, 213001 (2016).
- [25] D. Dong, C. Chen, B. Qi, I. R. Petersen, and F. Nori, *Sci. Rep.* **5**, 7873 (2014).
- [26] A. Sprl, T. Schulte-Herbrüggen, S. J. Glaser, V. Bergholm, M. J. Storz, J. Ferber, and F. K. Wilhelm, *Phys. Rev. A* **75**, 12302 (2007).
- [27] J. L. Allen, R. Kosut, J. Joo, P. Leek, and E. Ginossar, *Phys. Rev. A* **95**, 42325 (2017).
- [28] S. Montangero, T. Calarco, and R. Fazio, *Phys. Rev. Lett.* **99**, 170501 (2007).
- [29] S. van Frank, M. Bonneau, J. Schmiedmayer, S. Hild, C. Gross, M. Cheneau, I. Bloch, T. Pichler, A. Negretti, T. Calarco, and S. Montangero, *Scientific Reports* **6**, 34187 (2016).
- [30] S. van Frank, A. Negretti, T. Berrada, R. Bücker, S. Montangero, J.-F. Schaff, T. Schumm, T. Calarco, and

- J. Schmiedmayer, *Nat. Commun.* **5**, 4009 (2014).
- [31] J. Scheuer, X. Kong, R. S. Said, J. Chen, A. Kurz, L. Marseglia, J. Du, P. R. Hemmer, S. Montangero, T. Calarco, B. Naydenov, and F. Jelezko, *New J. Phys.* **16**, 93022 (2014).
- [32] F. Caruso, S. Montangero, T. Calarco, S. F. Huelga, and M. B. Plenio, *Phys. Rev. A* **85**, 42331 (2012).
- [33] S. Rosi, A. Bernard, N. Fabbri, L. Fallani, C. Fort, M. Inguscio, T. Calarco, and S. Montangero, *Phys. Rev. A* **88**, 21601 (2013).
- [34] I. Brouzos, A. Streltsov, A. Negretti, R. Said, T. Caneva, S. Montangero, and T. Calarco, *Phys. Rev. A* **92**, 062110 (2015).
- [35] T. Caneva, T. Calarco, R. Fazio, G. Santoro, and S. Montangero, *Phys. Rev. A* **84**, 012312 (2011).
- [36] I. M. de Sousa and A. V. Dodonov, *J. Phys. A: Math. Theor.* **48**, 245302 (2015); D. S. Veloso and A. V. Dodonov, *J. Phys. B: At. Mol. Opt. Phys.* **48**, 165503 (2015).
- [37] B. Bonnard, O. Cots, S. J. Glaser, M. Lapert, D. Sugny, and Y. Zhang, *IEEE Transaction On Automatic Control*, Vol. 57, No. 8 (2012).
- [38] N. Rach, M. M. Müller, T. Calarco, and S. Montangero, *Phys. Rev. A* **92**, 062343 (2015).
- [39] P. Doria, T. Calarco, and S. Montangero, *Phys. Rev. Lett.* **106**, 190501 (2011); T. Caneva, T. Calarco, and S. Montangero, *Phys. Rev. A* **84**, 22326 (2011).
- [40] S. Lloyd and S. Montangero, *Phys. Rev. Lett.* **113**, 10502 (2014).
- [41] F. Frank, T. Unden, J. Zoller, R. Said, T. Calarco, S. Montangero, B. Naydenov, and F. Jelezko, arXiv:1704.06514
- [42] S. Mavadia, V. Freq, J. Sastrawan, S. Dona, and M. Biercuk, *Nature Comm.* **8**, 14106 (2017).
- [43] D. Lu, K. Li, J. Li, H. Katiyar, A. J. Park, G. Feng, T. Xin, H. Li, G. Long, A. Brodutch, J. Baugh, B. Zeng, and R. Laflamme, arXiv:1701.01198.
- [44] R. L. Kosut, M. D. Grace, and C. Brif, *Phys. Rev. A* **88**, 52326 (2013).
- [45] M. Hofheinz, E. M. Weig, M. Ansmann, R. C. Bialczak, E. Lucero, M. Neeley, A. D. O'Connell, H. Wang, J. M. Martinis, and A. N. Cleland, *Nature* **454**, 310 (2008).
- [46] F. Angaroni, G. Benenti, and G. Strini, *Eur. Phys. J. D* **70**, 225 (2016).
- [47] G. Benenti, S. Siccardi, and G. Strini, *Eur. Phys. J. D* **68**, 139 (2014).
- [48] V. Mukherjee, A. Carlini, A. Mari, T. Caneva, S. Montangero, T. Calarco, R. Fazio, and V. Giovannetti, *Phys. Rev. A* **88**, 062326 (2013).